Electronic Supplementary Material (ESI) for Dalton Transactions.

Bimetallic nickel complexes containing imidazole-based phenolate ligands as efficient catalysts for copolymerization of carbon dioxide with epoxides

Han-Fang Hsu, Guan-Lin Liu, Yu-Chia Su and Bao-Tsan Ko*

Department of Chemistry, National Chung Hsing University, Taichung 402, Taiwan

Scheme S1 Synthetic pathways of ligand precursors.

Scheme S2 Selected bimetallic complexes based on amino-phenolate ligands and their catalytic performances for CO_2/CHO copolymerization.

Fig. S1 Mass spectrum of dinuclear nickel complex **1** was obtained using positive electron spray ionization (ESI^+) technique.

Fig. S2 Molecular structure of complex **2** (30% probability level). All hydrogen atoms (except those of the coordinated water) have been omitted for clarity.

Fig. S3 Molecular structure of complex **3** (30% probability level). All hydrogen atoms (except those of the coordinated water) have been omitted for clarity.

Fig. S4 Molecular structure of complex **4** (30% probability level). All hydrogen atoms (except those of the coordinated water) have been omitted for clarity.

Fig. S5 Molecular structure of complex **5** (30% probability level). All hydrogen atoms (except those of the coordinated water) have been omitted for clarity.

Fig. S6 Molecular structure of complex **6** (30% probability level). All hydrogen atoms (except those of the coordinated water) have been omitted for clarity.

Fig. S7 Molecular structure of complex **10** (30% probability level). All hydrogen atoms have been omitted for clarity.

Fig. S8 The plot of Mn (■) and *Đ* (▲) (determined from GPC analysis) *versus* CHO conversion for CO_2-copolymerization of CHO using dinickel complex **1** as the catalyst ($[CHO]_0/[\mathbf{1}]_0$ = 1600) at 120 °C and 300 psi initial CO_2 pressure.

Fig. S9 (a) GPC traces for the generated PCHC having a bimodal molecular weight distribution mediated by dinickel complex **1** (Table 3, entry 5). (b) GPC traces for the produced PCHC polyol having a unimodal molecular weight distribution mediated by Ni complex **1** (Table 4, entry 1).

Fig. S10 ^{1}H NMR spectrum of the purified copolymer mediated by using dinickel complex **1** in the presence of CHD (Table 4, entry 1) in $CDCl_3$. The peak at δ 4.65 ppm is assigned to the methine protons of repeated units in PCHC as well as the peaks at δ 4.37 and 3.56 ppm are assigned to methine protons that are adjacent to end-capped carbonate and hydroxy in PCHC, respectively.

Fig. S11 MALDI-TOF spectrum of the generated PCHC polyol promoted by Ni complex **1** on the addition of CHD as the CTA (Table 4, entry 1).

Fig. S12 The plot of TOFs with diverse initial CO_2 pressures (200, 250, 300 and 350 psi) using dinickel complex **1** (0.0625 mol%) at 120 °C for 1 h.

Table S1 CO_2/CHO Copolymerization catalyzed by using dinickel complex **1** under various initial CO_2 pressures for 1 h

Table S2 Kinetic studies of CO_2/CHO copolymerization mediated by dinickel complex **1** at diverse monomer-to-catalyst ratio (1200, 1600, 2000, 2400, 2800 and 5000)[a]

Table S3 Kinetic parameters for CO_2/CHO copolymerization mediated by dinickel complex **1** at various catalyst concentrations

Table S4 Crystallographic data of complexes **1**–**10**

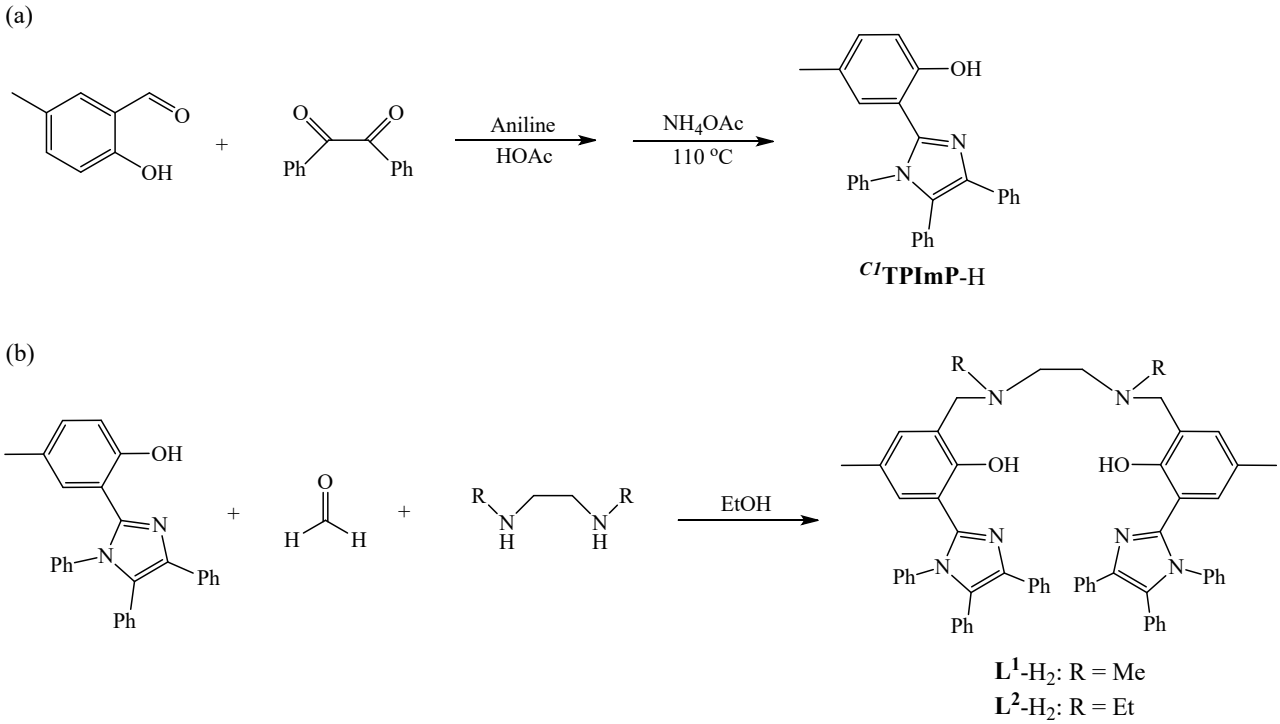

Scheme S1 Synthetic pathways of ligand precursors.

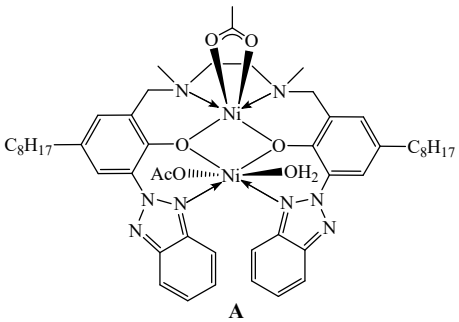

A

TOF = 204 h^{-1}

[120 °C, 300 psi, 0.0625 mol%, 4 h][34]

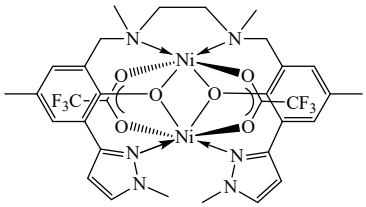

B

TOF = 144 h^{-1}

[140 °C, 300 psi, 0.0625 mol%, 6 h][35]

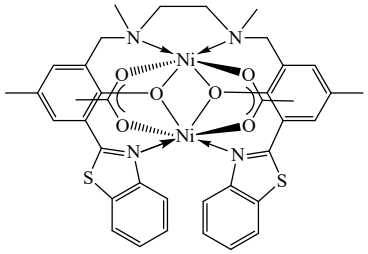

C

TOF = 212 h^{-1}

[120 °C, 300 psi, 0.0625 mol%, 4 h][36]

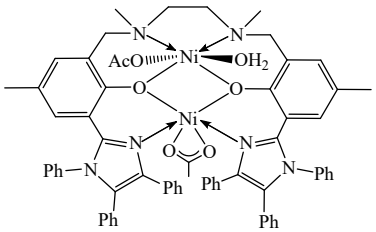

1

TOF = 496 h^{-1}

[120 °C, 300 psi, 0.0625 mol%, 2 h]

(This work)

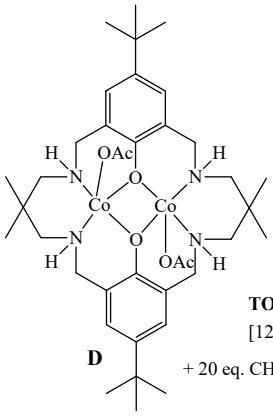

D

TOF = 4200 h^{-1}

[120 °C, 20 bar, 0.05 mol%][20]

+ 20 eq. CHD

Scheme S2 Selected bimetallic complexes based on amino-phenolate ligands and their catalytic performances for CO_2/CHO copolymerization.

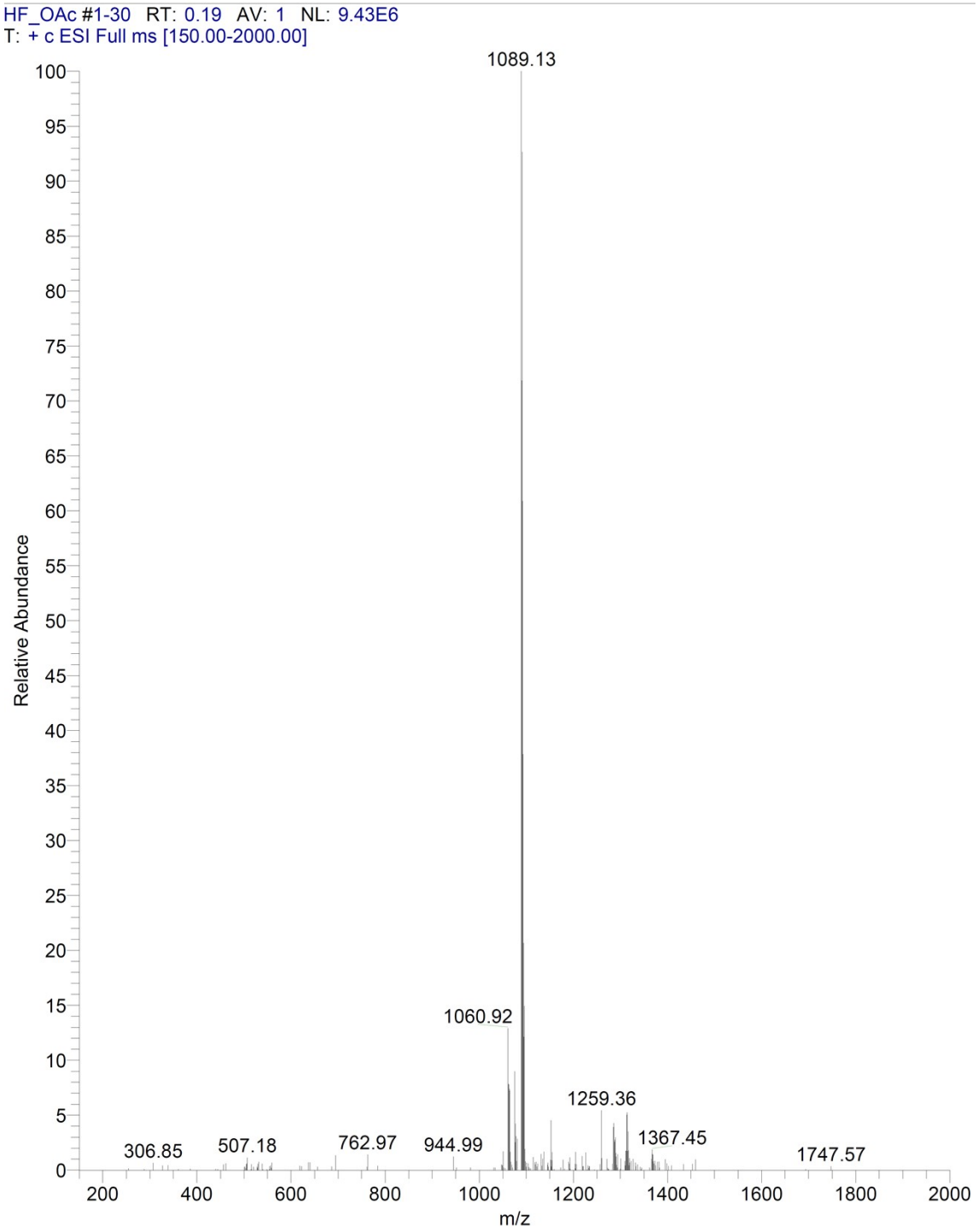

Fig. S1 Mass spectrum of dinuclear nickel complex **1** was obtained using positive electron spray ionization (ESI^+) technique.

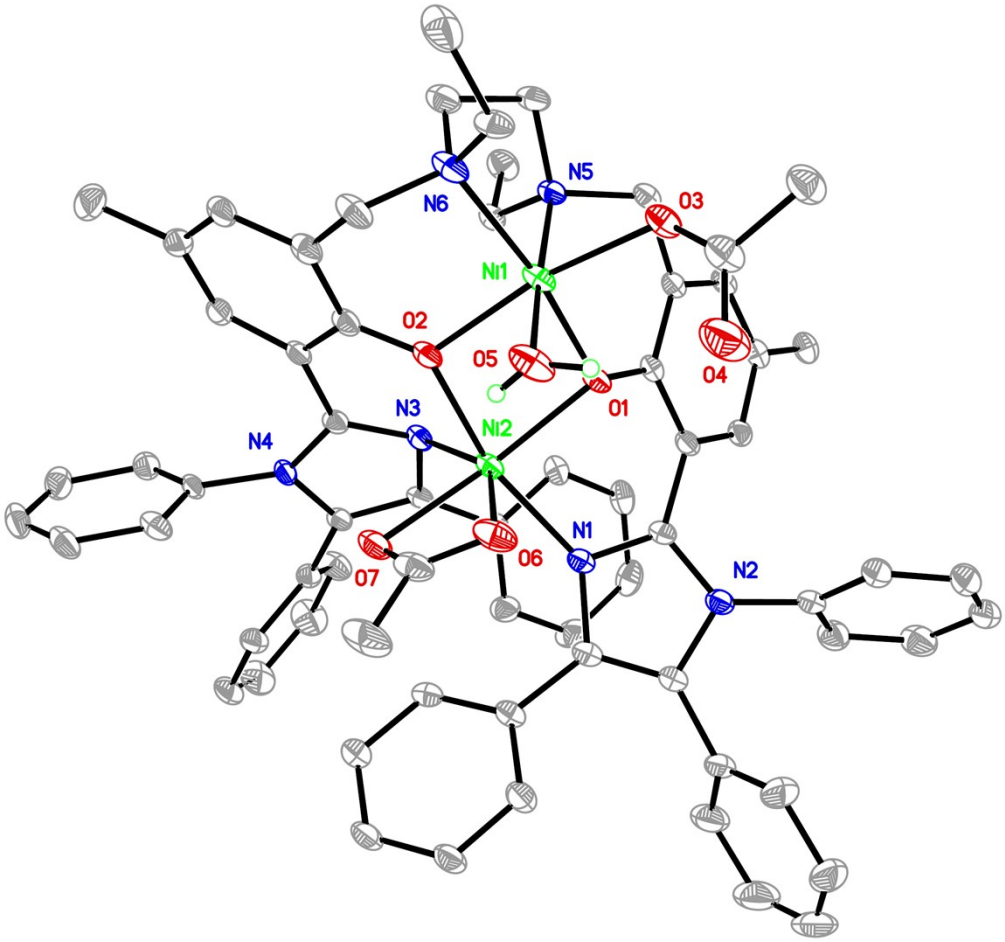

Fig. S2 Molecular structure of complex **2** (30% probability level). All hydrogen atoms (except those of the coordinated water) have been omitted for clarity.

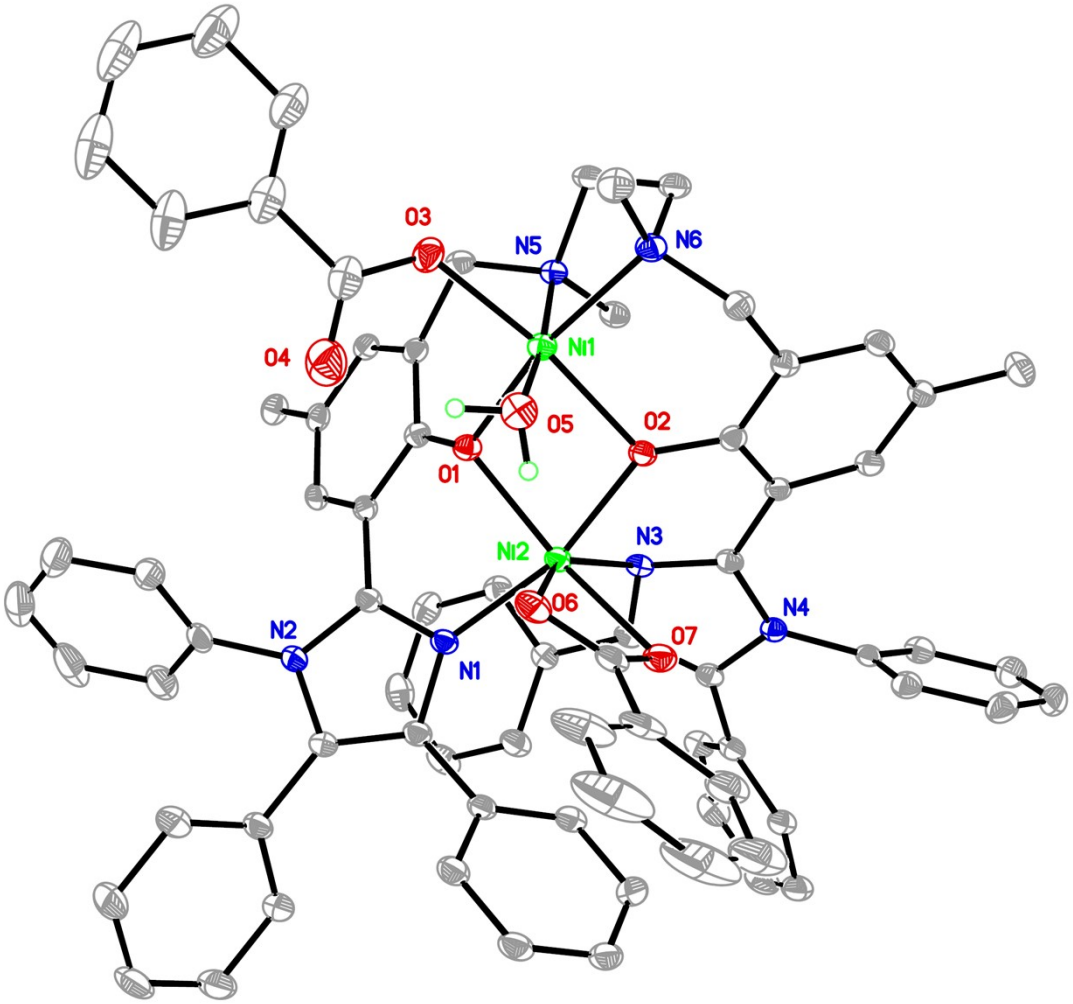

Fig. S3 Molecular structure of complex **3** (30% probability level). All hydrogen atoms (except those of the coordinated water) have been omitted for clarity.

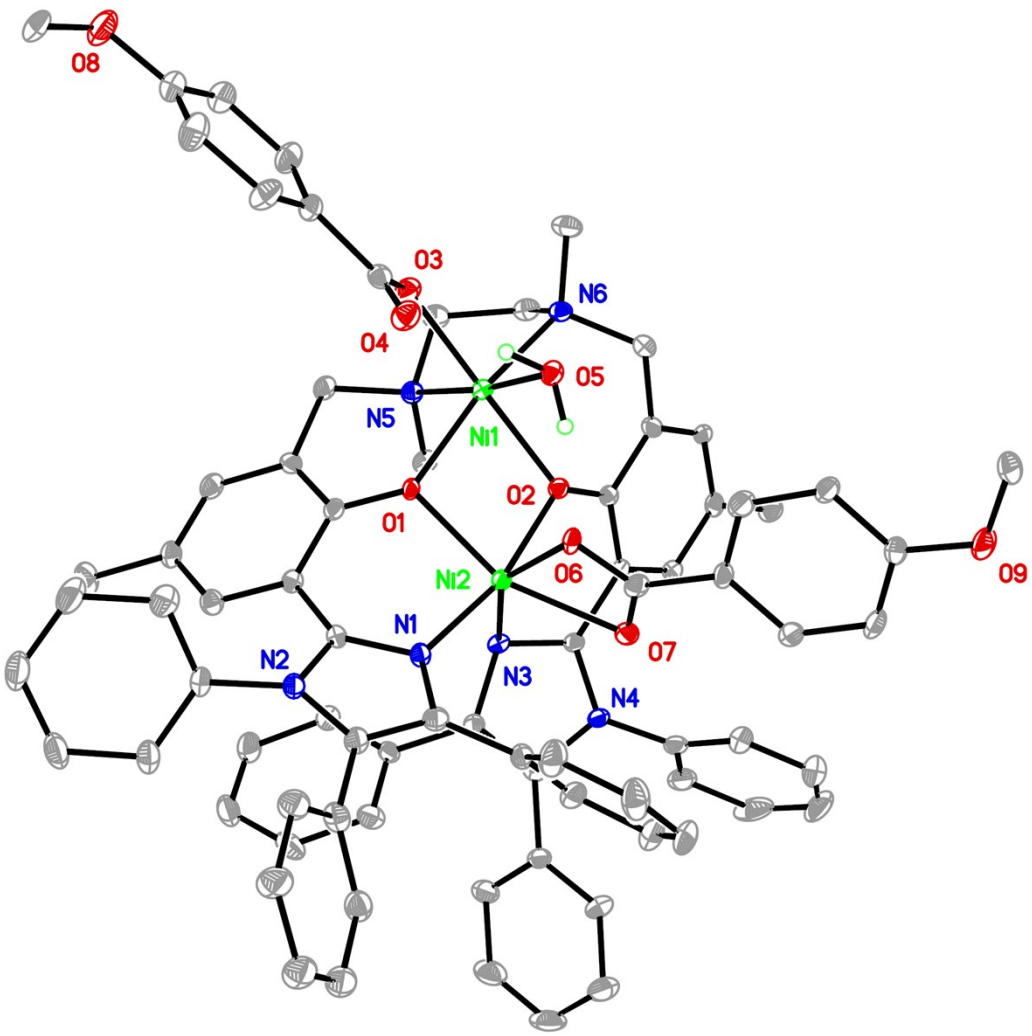

Fig. S4 Molecular structure of complex **4** (30% probability level). All hydrogen atoms (except those of the coordinated water) have been omitted for clarity.

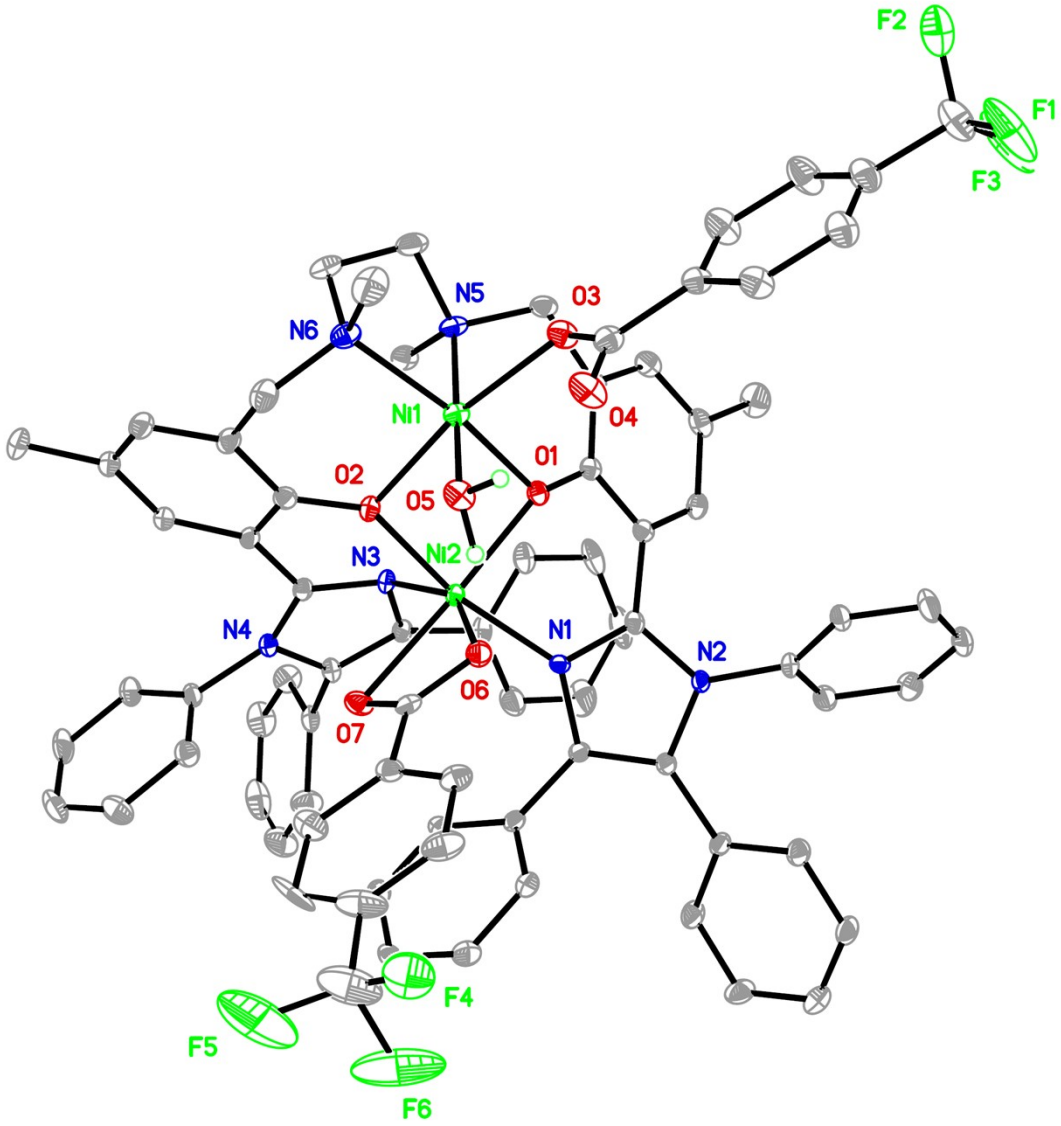

Fig. S5 Molecular structure of complex **5** (30% probability level). All hydrogen atoms (except those of the coordinated water) have been omitted for clarity.

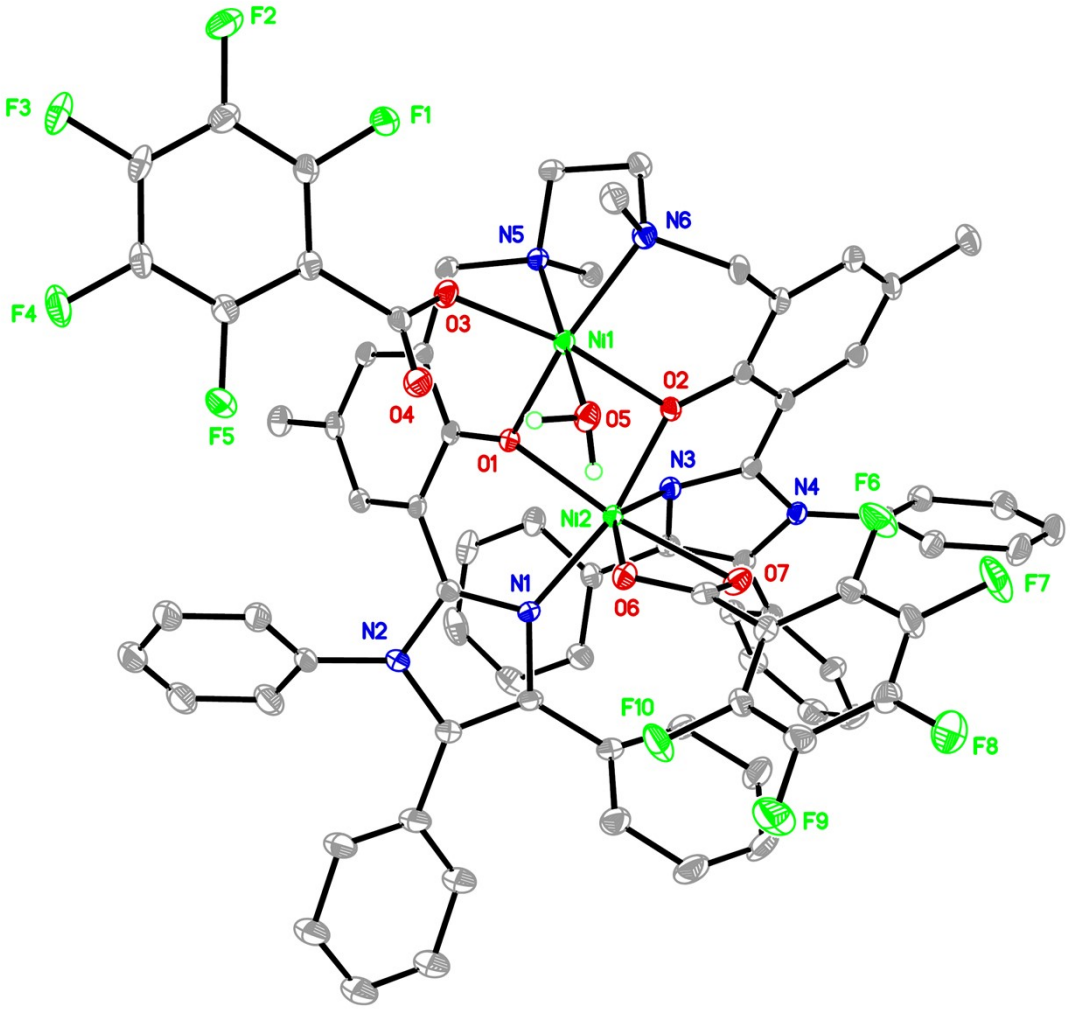

Fig. S6 Molecular structure of complex **6** (30% probability level). All hydrogen atoms (except those of the coordinated water) have been omitted for clarity.

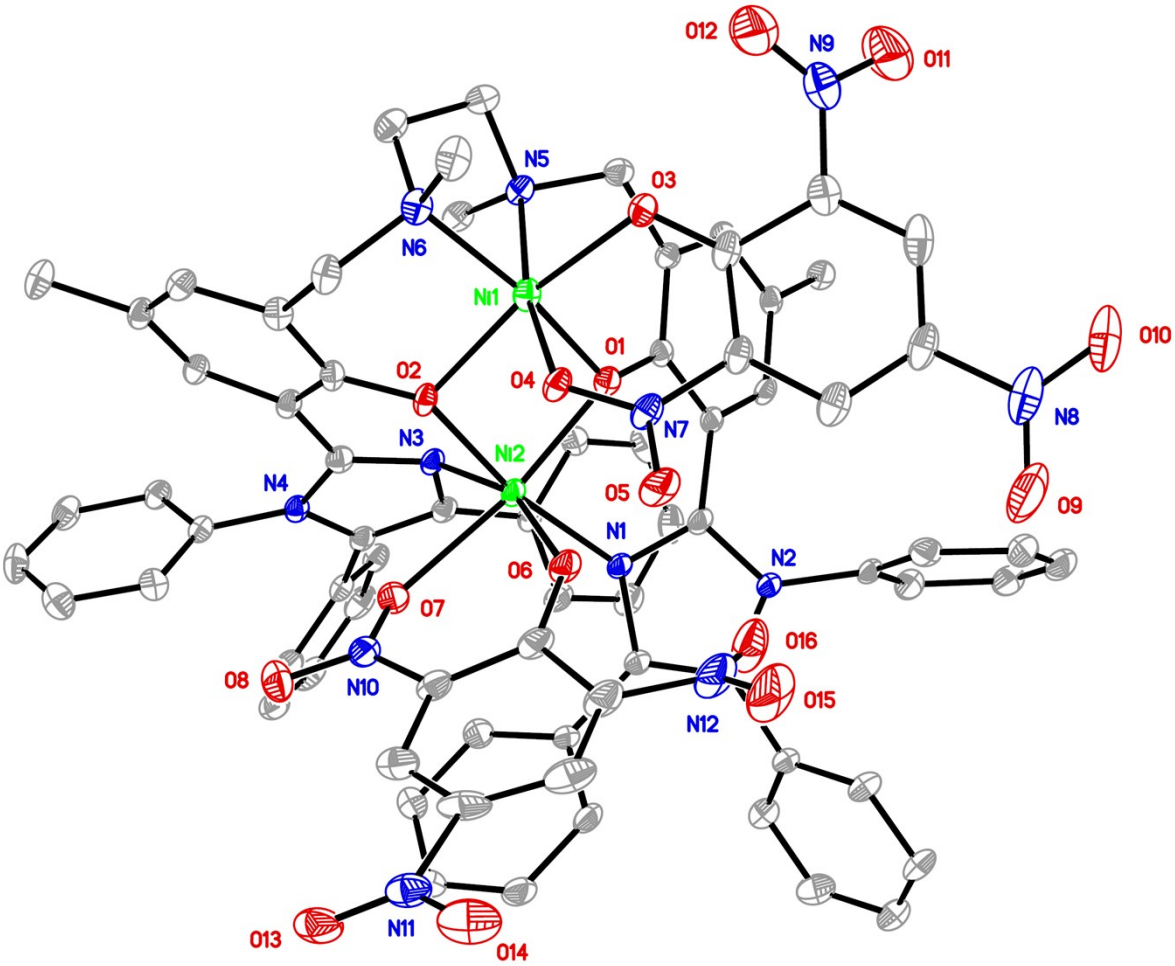

Fig. S7 Molecular structure of complex **10** (30% probability level). All hydrogen atoms have been omitted for clarity.

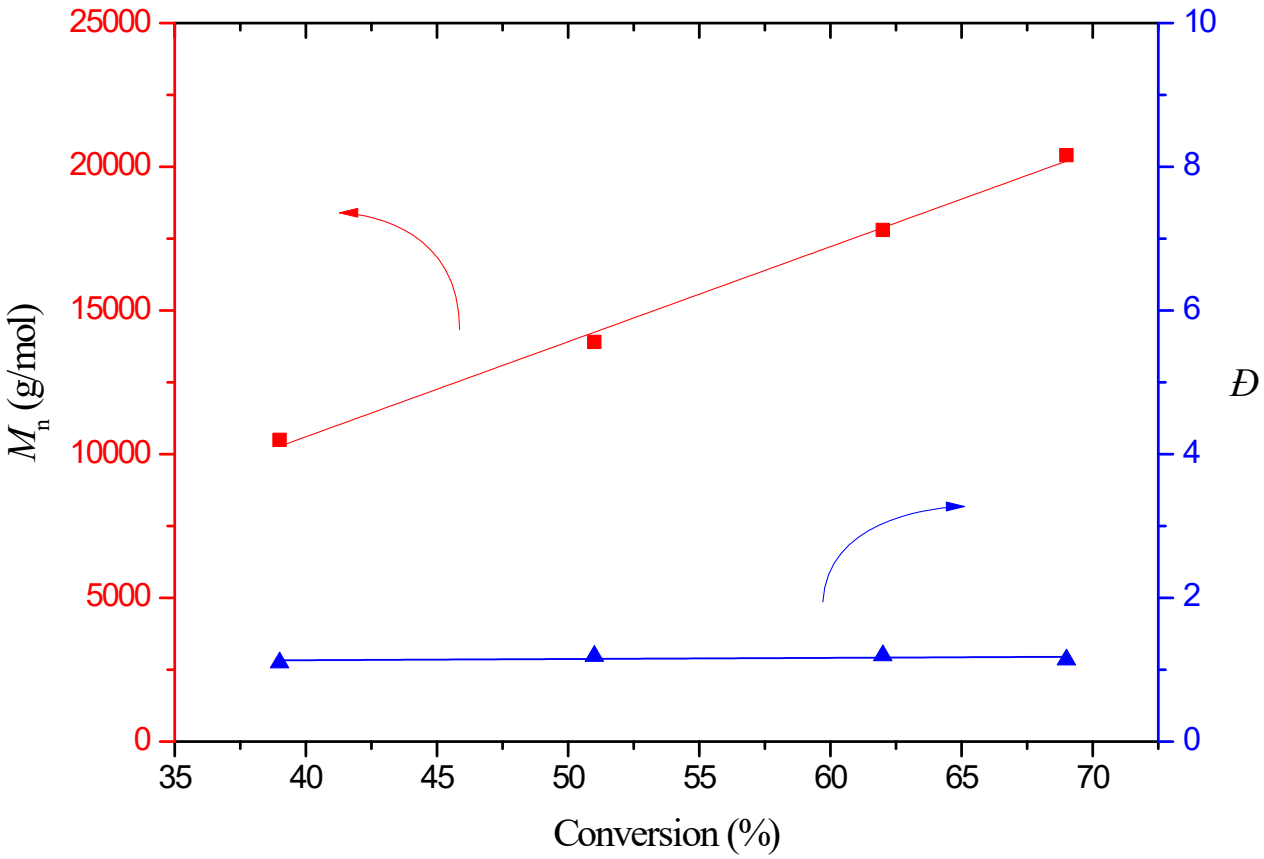

Fig. S8 The plot of Mn (■) and *Đ* (▲) (determined from GPC analysis) *versus* CHO conversion for CO_2-copolymerization of CHO using dinickel complex **1** as the catalyst ($[CHO]_0/[\mathbf{1}]_0 = 1600$) at 120 °C and 300 psi initial CO_2 pressure.

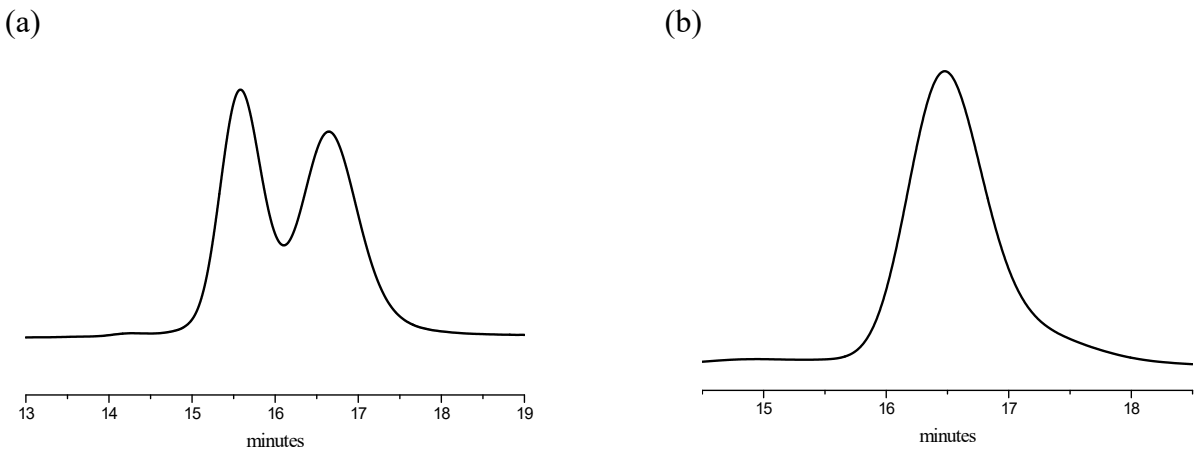

Fig. S9 (a) GPC traces for the generated PCHC having a bimodal molecular weight distribution mediated by dinickel complex **1** (Table 3, entry 5). (b) GPC traces for the produced PCHC polyol having a unimodal molecular weight distribution mediated by Ni complex **1** (Table 4, entry 1).

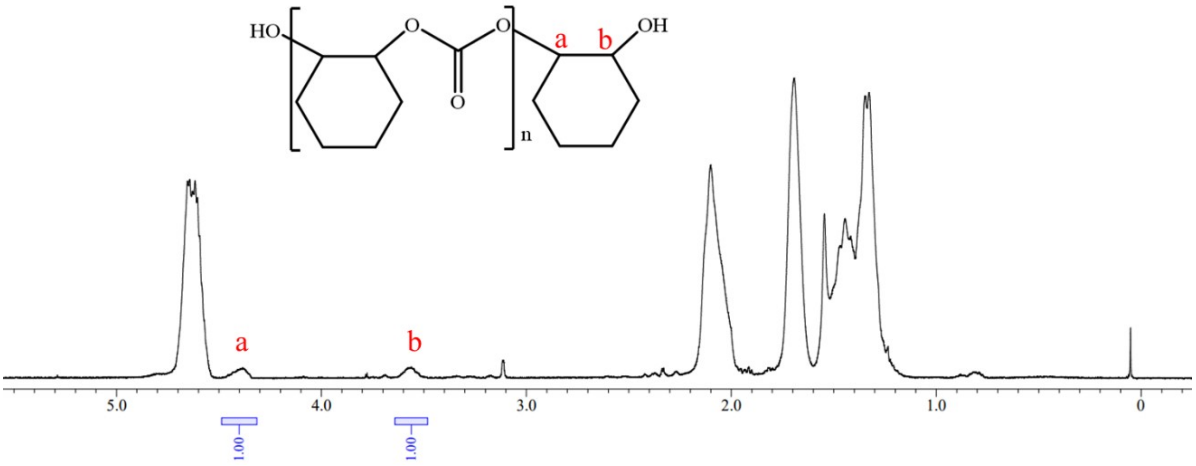

Fig. S10 ^{1}H NMR spectrum of the purified copolymer mediated by using dinickel complex **1** in the presence of CHD (Table 4, entry 1) in $CDCl_3$. The peak at δ 4.65 ppm is assigned to the methine protons of repeated units in PCHC as well as the peaks at δ 4.37 and 3.56 ppm are assigned to methine protons that are adjacent to end-capped carbonate and hydroxy in PCHC, respectively.

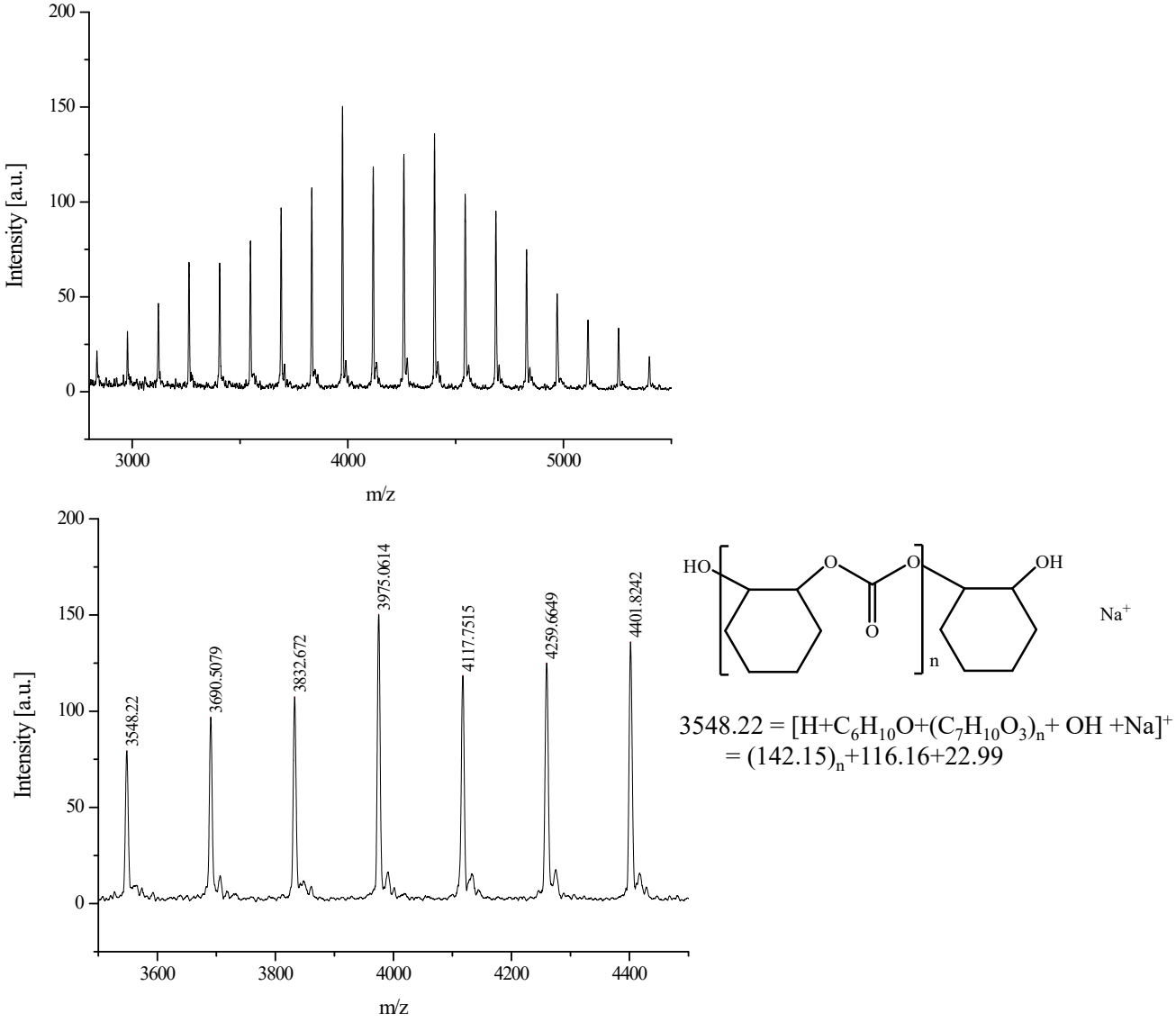

Fig. S11 MALDI-TOF spectrum of the generated PCHC polyol promoted by Ni complex **1** on the addition of CHD as the CTA (Table 4, entry 1).

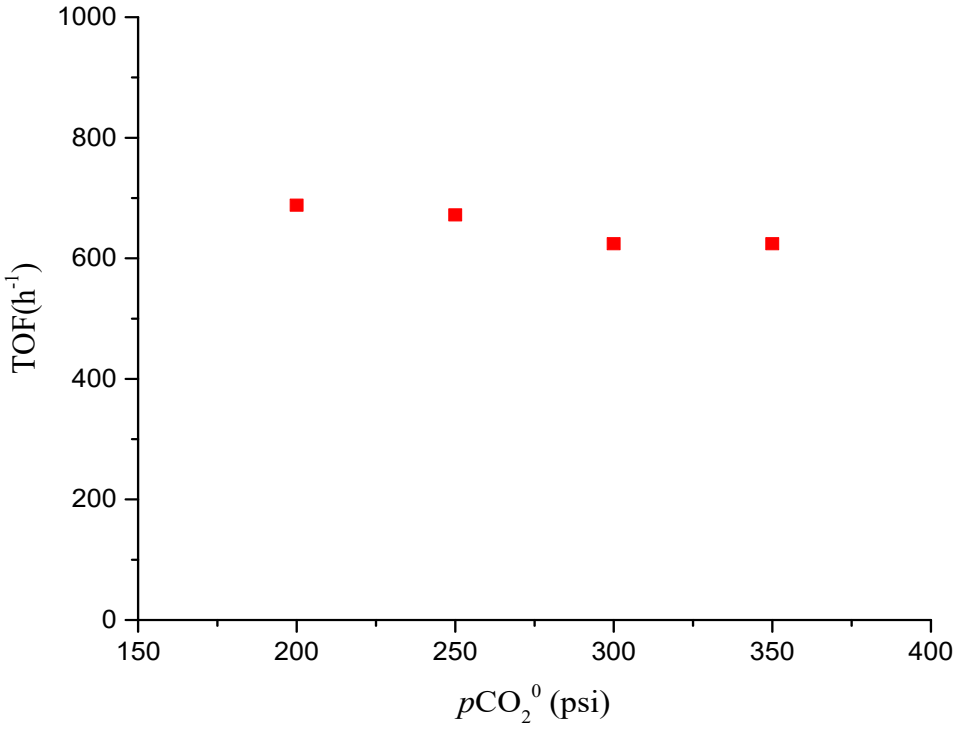

Fig. S12 The plot of TOFs with diverse initial CO_2 pressures (200, 250, 300 and 350 psi) using dinickel complex **1** (0.0625 mol%) at 120 °C for 1 h.

Table S1 CO_2/CHO Copolymerization catalyzed by using dinickel complex **1** under various initial CO_2 pressures for 1 h

Entry	Pressure /psi	% CHO Conv.[a]	% Copolymer[a] (%CO_3 linkages)[b]	TON[c]	TOF /h^{-1}[d]
S1	200	43	96(>99)	688	688
S2	250	42	96(>99)	672	672
S3	300	39	>99(>99)	624	624
S4	350	39	>99(>99)	624	624

Copolymerization conditions: 0.0625 mol% catalyst, Temp. = 120 °C. [a]Based on ^{1}H NMR analysis of the reaction mixture. [b]Based on ^{1}H NMR determination of the purified copolymers. [c]TON = number of moles of CHO consumed per mole of catalyst. [d]TOF = TON per hour.

Table S2 Kinetic studies of CO_2/CHO copolymerization mediated by dinickel complex **1** at diverse monomer-to-catalyst ratio (1200, 1600, 2000, 2400, 2800 and 5000)[a]

Entry	$[CHO]_0$:$[\mathbf{1}]_0$	Time/h	%CHO Conv.[b]	$\ln([CHO]_0/[CHO]_t)$
S1	1200	0.5	34	0.416
S2	1200	0.75	42	0.545
S3	1200	1	54	0.777
S4	1200	1.5	67	1.109
S5	1600	1	39	0.494
S6	1600	1.5	51	0.713
S7	1600	2	62	0.968
S8	1600	2.5	69	1.171
S9	2000	1	35	0.431
S10	2000	1.5	44	0.580
S11	2000	2	54	0.777
S12	2000	2.5	63	0.994
S13	2400	1	25	0.288
S14	2400	1.5	36	0.446
S15	2400	2	45	0.598
S16	2400	2.5	52	0.734
S17	2800	1	22	0.248
S18	2800	1.5	31	0.371
S19	2800	2	39	0.494
S20	2800	2.5	45	0.598
S21	5000	2	22	0.248

S22	5000	3	32	0.386
S23	5000	4	39	0.494
S24	5000	5	45	0.598

[a]Copolymerization conditions: 100.0 mmol CHO, 120 °C, pCO_2^0 = 300 psi. [b]Based on ^{1}H NMR analysis of the reaction mixture.

Table S3 Kinetic parameters for CO_2/CHO copolymerization mediated by dinickel complex **1** at various catalyst concentrations

Entry	$[CHO]_0$:$[\mathbf{1}]_0$	Observed rate coefficient, k_{obs} (h^{-1})[a]	$\ln(k_{obs})$	catalyst concentrations [**1**] (M)[b]	ln[**1**]
S1	1200	0.7099	–0.343	8.333 x 10^{-3}	–4.788
S2	1600	0.4570	–0.783	6.250 x 10^{-3}	–5.075
S3	2000	0.3774	–0.974	5.000 x 10^{-3}	–5.298
S4	2400	0.2981	–1.210	4.167 x 10^{-3}	–5.481
S5	2800	0.2343	–1.451	3.571 x 10^{-3}	–5.635
S6	5000	0.1157	–2.157	2.000 x 10^{-3}	–6.215

[a]Calculated from the slope of the fitted regression line of Fig. 6a.

[b]A fixed amount of CHO (100.0 mmol) was used.

Table S4 Crystallographic data of complexes **1**–**10**

	1·0.5[C_3H_6O]	**2**·1[H_2O]·1.5[CH_2Cl_2]	**3**·1[C_6H_{14}]·1.5[CH_2Cl_2]	**4**·1[H_2O] 2[C_6H_{14}]
Temp (K)	150.15	181	150	150.15
Crystal system	Monoclinic	Trigonal	Triclinic	Monoclinic
Space group	$P2_1/n$	R-3	P-1	$P2_1/n$
a (Å)	12.5633(11)	38.1705(19)	14.4235(18)	15.0623(12)
b (Å)	32.882(3)	38.1705(19)	16.341(2)	47.324(4)
c (Å)	14.9737(12)	22.8167(10)	17.149(2)	11.6909(8)
α (deg)	90	90	78.062(4)	90
β (deg)	107.869(3)	90	78.226(4)	112.230(2)
γ (deg)	90	120	73.085(5)	90
V(Å^3)	5887.3(9)	28790(3)	3738.6(9)	7714.0(10)
Z	4	18	2	4
D_{calc}(Mg/m^3)	1.351	1.393	1.338	1.329
μ (Mo Kα)(mm^{-1})	0.701	0.775	0.670	0.554
F(000)	2512	12618	1578	3272
Reflections collected	80197	135930	50721	73662
No. of parameters	762	777	872	927
Indep. reflns (R_{int})	10338 (0.0973)	11253 (0.0851)	13111 (0.0345)	13515 (0.0746)
$R1[I > 2\sigma(I)]$	0.0967	0.0498,	0.0392	0.0778
w$R2$ $[I > 2\sigma(I)]$	0.2161	0.1189	0.1004	0.1687
Goodness-of-fit on F^2	1.298	1.073	1.048	1.107

Table S4 Crystallographic data of complexes **1**–**10** (Cont'd)

	5·2[$C_4H_{10}O$]	**6**·2[C_6H_{14}]	**7**·2[H_2O]·3[CH_2Cl_2]	**8**·1[CH_2Cl_2]·2[CH_3OH]
Temp (K)	150	150	150.15	150
Crystal system	Monoclinic	Triclinic	Triclinic	Triclinic
Space group	$P2_1/n$	P-1	P-1	P-1
a (Å)	12.1166(8)	14.930(3)	12.6449(17)	11.4310(14)
b (Å)	15.1812(11)	15.514(3)	13.4163(19)	13.7228(16)
c (Å)	40.797(3)	17.571(4)	22.200(3)	21.986(3)
α (deg)	90	98.726(7)	87.747(4)	85.922(4)
β (deg)	95.998(2)	97.283(7)	74.480(4)	74.860(5)
γ (deg)	90	107.756(7)	72.929(4)	84.965(4)
V(Å^3)	7463.3(9)	3766.0(12)	3465.8(8)	3312.1(7)
Z	4	2	2	2
D_{calc}(Mg/m^3)	1.403	1.451	1.485	1.423
μ (Mo Kα)(mm^{-1})	0.584	0.588	0.850	0.756
F(000)	3296	1712	1592	1476
Reflections collected	98493	52911	40229	43590
No. of parameters	911	915	797	808
Indep. reflns (R_{int})	13088 (0.0822)	13208 (0.0535)	12114 (0.1011)	11577 (0.0477)
$R1[I > 2\sigma(I)]$	0.0679	0.0379	0.0955	0.0637
w$R2$ $[I > 2\sigma(I)]$	0.1578	0.0977	0.2416	0.1544
Goodness-of-fit on F^2	1.179	1.037	1.056	1.059

Table S4 Crystallographic data of complexes **1**–**10** (Cont'd)

	9·1[H_2O]	**10**·2[CH_2Cl_2]
Temp (K)	150	150
Crystal system	Triclinic	Triclinic
Space group	*P*-1	*P*-1
a (Å)	13.7649(7)	14.930(3)
b (Å)	13.7918(7)	15.514(3)
c (Å)	17.4684(9)	17.571(4)
α (deg)	80.804(2)	98.726(7)
β (deg)	87.163(2)	97.283(7)
γ (deg)	80.733(2)	107.756(7)
V(Å^3)	3229.9(3)	3766.0(12)
Z	2	2
D_{calc}(Mg/m^3)	1.457	1.451
μ (Mo Kα)(mm^{-1})	0.659	0.588
F(000)	1472	1712
Reflections collected	50206	52911
No. of parameters	904	915
Indep. reflns (R_{int})	13155 (0.0420)	13208 (0.0535)
$R1[I > 2\sigma(I)]$	0.0484	0.0379
w$R2$ $[I > 2\sigma(I)]$	0.0979	0.0977
Goodness-of-fit on F^2	1.087	1.037